Polymer Journal (2022) 54:455–464
https://doi.org/10.1038/s41428-021-00604-w

FOCUS REVIEW

Self-assembly of carbohydrate-based block copolymer systems: glyconanoparticles and highly nanostructured thin films

Hong Li[1] · Muhammad Mumtaz[1] · Takuya Isono[2] · Toshifumi Satoh[2] · Wen-Chang Chen[3,4] · Redouane Borsali[1]

Received: 31 October 2021 / Revised: 17 November 2021 / Accepted: 19 November 2021 / Published online: 14 January 2022

Abstract

Carbohydrates constitute a sustainable source of materials that has attracted growing interest due to their "green" aspects, biocompatibility, biodegradability and biorecognition properties. Their industrial applications at the macroscopic scale offer new solutions for biobased materials, and they have been applied in different sectors, such as cosmetics, health, packaging, or microelectronics. To gain more understanding and incorporate these systems into new challenges/applications and devices (e.g., bionanoelectronics) in response to the transition to a biobased economy, it is of great importance to control their self-assembly at the nanoscale. This has been the aim of our work during the past decade—we have used "click chemistry" and developed a new class of linear carbohydrate-based (so-called high χ) diblock copolymer systems resulting, via self-assembly, in highly nanostructured sub-10-nm-resolution thin films. In this focused review, we summarize some recent work illustrating the self-assembly properties leading to the design of glyconanoparticles and highly nanostructured thin films potentially of great importance in different applications and biomarkers.

Introduction

The major interest in block copolymer (BCP) nanostructured materials and their manipulation in nanoscience derives from the promise of manipulating matter atom-by-atom and molecule-by-molecule to create the next generation of miniaturized devices with performances and functionalities that are orders of magnitude more efficient than those provided by current manufacturing technologies. Two general approaches, known as top-down and bottom-up strategies, are actually applied to the preparation of nanosized structures. The top-down strategy consists of "carving" a pre-existing macroscopic material through, for example, chemical, mechanical or optical processes (lithography) to obtain final materials with precisely designed shapes, dimensions and properties. The challenge facing the nanotechnology community today is the development of novel structures whose sizes and spacing are approaching a few nanometers. This can be accomplished via the so-called bottom-up approach, which consists of hierarchically assembling (chemically or physically) a finite number of elementary building blocks (atoms, molecules or macromolecules). In addition to the reduced number of steps associated with this strategy, it is reversible in most cases and allows the combination of different materials (minerals, metals, synthetic and natural polymers, etc.). Bottom-up methods can elaborate tailored and complex materials via self-assembly processes driven by chemical and/or physical forces with low-cost technology compared to standard techniques.

Self-assembly of BCP systems enables the low-cost design of well-defined nanometer-sized nanoparticles and periodic patterns that find potential applications in nanolithography, nanoscale device fabrication, production of porous materials, templating and patterning of (in)organic materials, which find important developments in catalysis, membrane separation, sensors, the semiconductor industry and storage technology [1–4]. The thermodynamics

✉ Redouane Borsali
borsali@cermav.cnrs.fr

[1] Univ. Grenoble Alpes, CNRS, CERMAV, 38000 Grenoble, France

[2] Faculty of Engineering, Hokkaido University, Sapporo 060-8628, Japan

[3] Advanced Research Center for Green Materials Science and Technology, National Taiwan University, Taipei 10617, Taiwan

[4] Department of Chemical Engineering, National Taiwan University, Taipei 10617, Taiwan

dictating the self-organization of a coil-coil BCP are well established [5].

Depending on the block incompatibility (Flory interaction parameter χ) and the BCP composition (weight fraction and polymerization degree), one can design suspensions of nanoparticles (spherical micelles, worm-like micelles and vesicles) in solution, and different morphologies can be generated in thin films, i.e., spherical domains, lamellar domains oriented perpendicular to the substrate, bicontinuous gyroids, and hexagonally packed cylinders oriented either perpendicular or parallel to the substrate. To date, the most studied and applied BCP systems thus far are poly (styrene)-b-poly(methyl methacrylate) (PS-b-PMMA) [6], poly(styrene)-b-poly(ethylene oxide) (PS-b-PEO) [7], poly (styrene)-b-poly(lactide) (PS-b-PLA) [8], and poly(styrene)-b-poly(2-vinylpyridyne) (PS-b-P2VP) [9]. These model systems have enabled us to reach some of the most advanced knowledge and applications of BCP self-assembly as well as most innovative conceptual designs for their application as nanostructured templates [10]. However, all of them have typical limitations and advantages (e.g., thickness, long period, long-range order, and degradability limitations as well as the necessity for surface "neutralization"), making them complementary systems for the community working on BCP self-assembly. In addition, other BCP structures, e.g., PS-b-poly(dimethylsiloxane) (PS-b-PDMS) [11], P2VP-b-PDMS [12], or star-shaped miktoarm BCPs [13], have also significantly contributed to the actual state-of-the-art BCP self-assembly.

In the last decade, many efforts have been devoted to developing high-χ (and thus low-N) BCPs to reach sub-10 nm nanopatterns [14]. This is motivated by the fact that smaller features can be accessed using materials with low polymerization degrees only if the χN product required for phase separation is compensated by a higher value of χ. This has been afforded by the careful design of new generations of BCP systems. Among others, significant examples of high-χ BCPs include PS-b-maltoheptaose (PS-b-MH, a pioneering example affording one of the lowest features reported to date: 5 nm) [15, 16], poly (trimethylsilylstyrene)-b-MH (PTMSS-b-MH) [17], PDMS-b-PMMA [18], poly(1,1-dimethyl silacyclobutane)-b-poly (methyl methacrylate) (PDMSB-b-PMMA) [19, 20], or poly (cyclohexylethylene)-b-PMMA [21].

This paper provides an overview of the design of glyconanoparticles [22–31] and thin films [32–62] obtained from the self-assembly of high-χ carbohydrate-based BCPs (PS-b-MH) and summarizes some significant results obtained by the group of Hokkaido University (T. Satoh, T. Isono), the group of National Taiwan University (W.-C. Chen), and the group of Univ. Grenoble Alpes (CNRS-CERMAV) (R. Borsali).

Characterization methods

Characterization

^{1}H NMR spectra of polymer samples were recorded on a Bruker Avance 400 MHz spectrometer with a frequency of 400.13 MHz and calibrated with the signal of deuterated solvent. Size exclusion chromatography (SEC) was performed at 40 °C using an Agilent 390 MDS system (290 LC pump injector, ProStar 510 column oven, 390 MDS refractive index detector) equipped with a Knauer Smartline UV detector 2500 and two Agilent Poly Pore PL1113–6500 columns (linear, 7.5 × 300 mm; particle size, 5 µm; exclusion limit, 200–2,000,000) in DMF containing lithium chloride (0.01 M) at a flow rate of 1.0 mL min^{-1}.

Typical systems such as polystyrene-*b*-maltoheptaose (PS-*b*-MH) are generally synthesized using the click reaction of azido-functionalized polystyrene (PS-N_3) with alkynyl functionalized maltoheptaose (MH) in DMF at 65 °C in the presence of copper nanopowder (Scheme 1).

As illustrated in Scheme 1, ω-hydroxyl-polystyrene (PS-OH) is first synthesized by anionic polymerization of styrene in toluene using *sec*-butyllithium as an initiator at 35 °C for 3 h. The reaction is then terminated by ethylene oxide, accompanied by the addition of degassed methanol. PS-OH is treated with *p*-toluenesufonyl chloride in the presence of

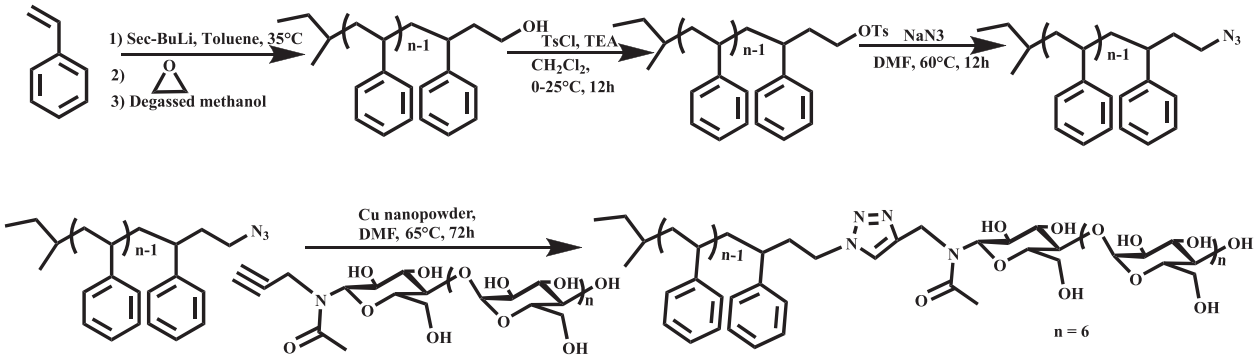

Scheme 1 Synthesis of polystyrene-b-maltoheptaose block copolymer

triethylamine (TEA) to obtain tosyl-functionalized polystyrene (PS-OTs), which is then treated with excess NaN_3 in DMF at 65 °C overnight to obtain azido-functionalized polystyrene (PS-N_3).

Block copolymer (BCP) synthesis protocols

PS-*b*-MH BCP synthesis is preceded by hydroxyl-terminated polystyrene (PS-OH), tosyl terminated polystyrene (PS-OTs) and azido-functionalized polystyrene (PS-N_3) preparation.

Synthesis of hydroxyl-terminated polystyrene (PS-OH)

Hydroxyl-terminated polystyrene is prepared by anionic polymerization of styrene accompanied by termination with ethylene oxide. The sample is characterized using ^{1}H NMR and SEC. M_n (^{1}H NMR) ~ 4500 g/mol, M_n (SEC, DMF) = 3800 g/mol.

Synthesis of azido-functionalized polystyrene (PS-N_3)

The azido-functionalized polystyrene is prepared in the following two steps: in the first step, polystyrene is dissolved in dried CH_2Cl_2 in a two-necked, round-bottom, flame-dried flask equipped with a magnetic stirrer, followed by the addition of trimethylamine. The temperature of the reaction is reduced to 0 °C by placing the flask in an ice bath. The white precipitate of azido-terminated polystyrene is filtered using a sintered glass funnel under vacuum and dried in a vacuum oven at 40 °C overnight, producing 8.0 g of solid product, with ~89% yield. The sample is characterized by ^{1}H NMR and SEC.

The displacement of signals at 3.3 ppm in ^{1}H NMR of PS-OTs (Fig. 1) due to -CH_2CH_2OH of PS-OH and the appearance of new peaks at 7.7 ppm corresponding to tosyl functional groups indicates the formation of tosyl-functionalized polystyrene. Finally, the complete disappearance of the signals at 7.7 ppm dedicated to tosyl function after treatment with NaN_3 confirms the formation of azido-functionalized polystyrene.

Synthesis of the polystyrene-block-maltoheptaose (PS-b-MH) block copolymer system

PS-*b*-MH is prepared by click chemistry of azido-functionalized PS and alkynyl-functionalized maltoheptaose. The solution is stirred under an argon atmosphere at 65 °C for 3 days. At the end of the reaction, the crude heterogeneous solution is diluted with THF and

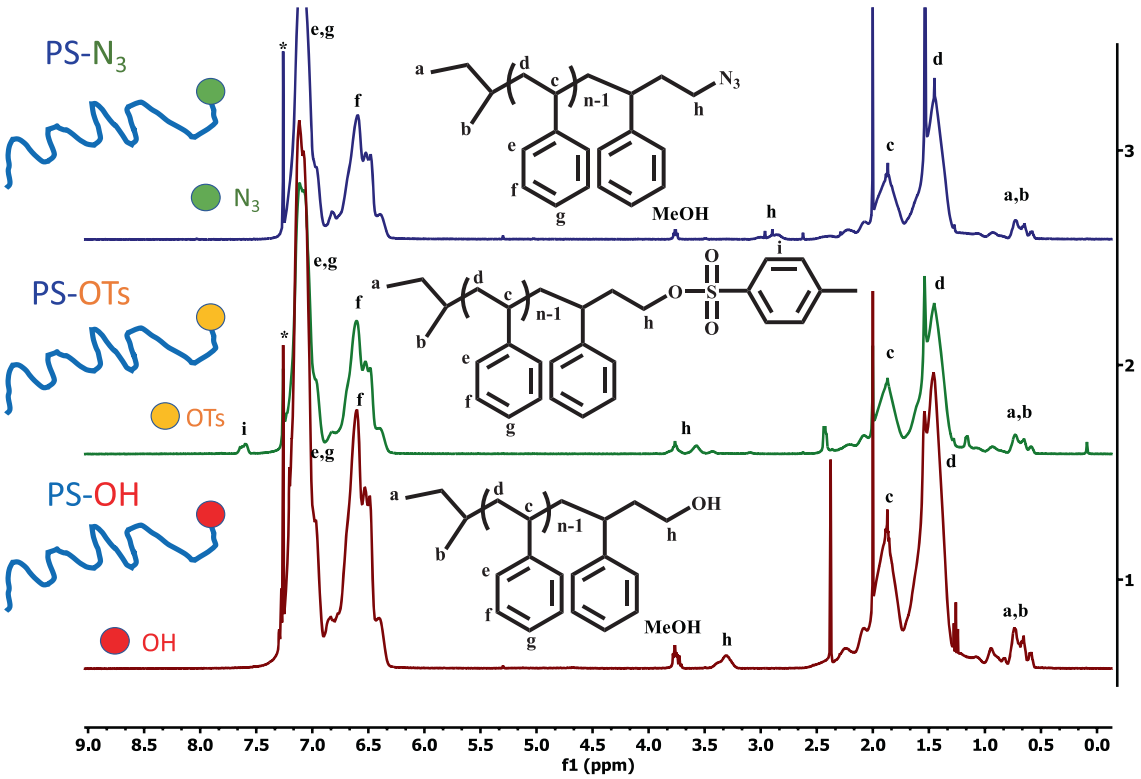

Fig. 1 ^{1}H NMR of (**a**) PS-OH, (**b**) PS-OTs and (**c**) PS-N_3 in $CDCl_3$ at 25 °C (400 MHz)

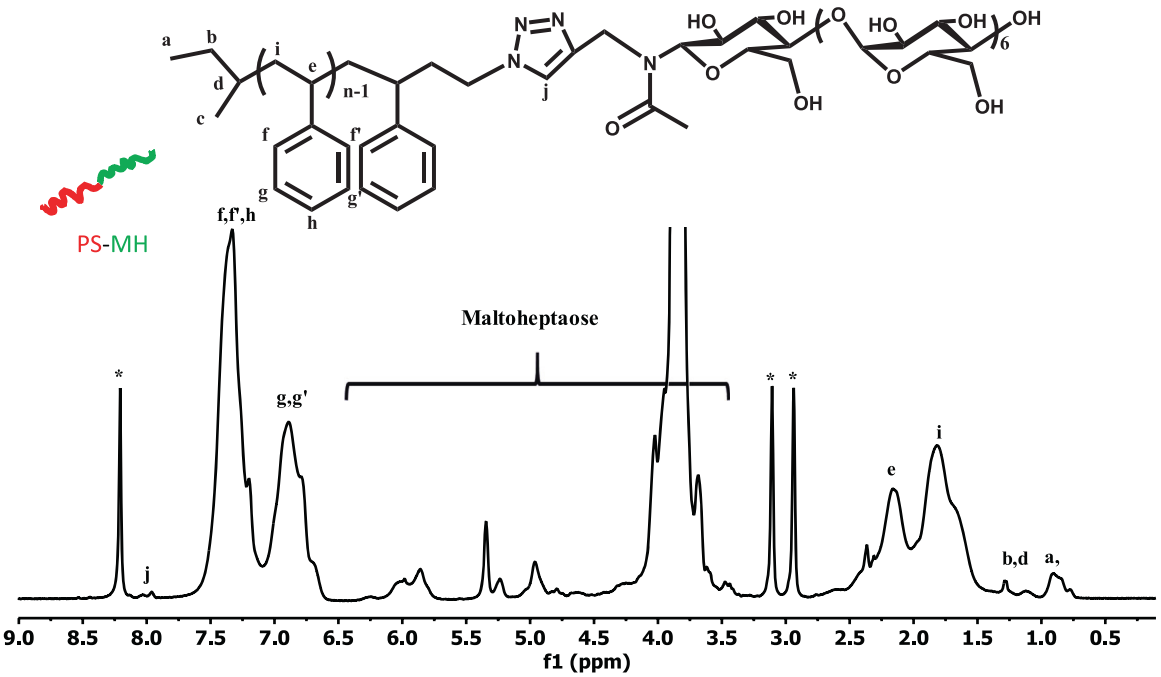

Fig. 2 ^{1}H NMR of PS-*b*-MH in DMF-d_7 at 25 °C (400 MHz)

filtered through diatomaceous earth. The unreacted polystyrene is removed by precipitation of the copolymer in a cyclohexane/heptane (60/40, v/v) mixture. The resulting white solid (~85% yield) is dried in vacuum at 40 °C overnight and characterized by ^{1}H NMR and SEC.

Typical NMR spectra of PS-*b*-MH are illustrated in Fig. 2. The presence of signals at 6.5–7.7 ppm due to polystyrene and 3.2–6.3 ppm dedicated to maltoheptaose in ^{1}H NMR of PS-*b*-MH in DMF-d_7 indicate the synthesis of block copolymers.

The complete shifting of peaks dedicated to MH and PS-N_3 in the SEC chromatogram (Fig. 3) toward higher molecular weights confirms the formation of PS-*b*-MH.

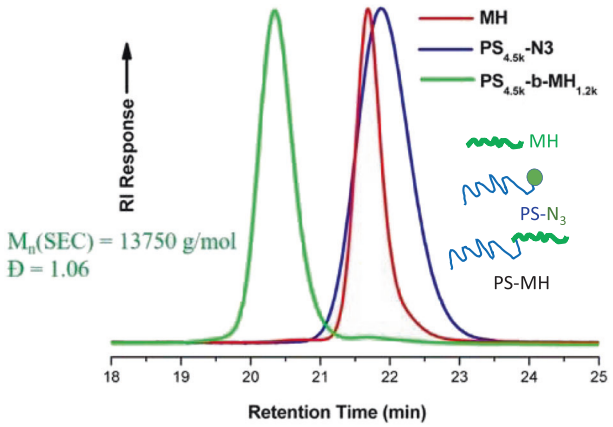

Fig. 3 SEC traces of $PS_{4.5k}$-N_3 (blue), $MH_{1.2k}$ (red) and $PS_{4.5k}$-*b*-$MH_{1.2k}$ (green)

Illustrations of typical results and discussion

Self-assembly in solution: glyconanoparticles

Glyconanoparticles are generally obtained using the nanoprecipitation technique: Dissolution of the copolymer system at different concentrations (illustration of PS-*b*-MH) in a cosolvent (organic solvent/water) solution (X:Y) v/v stirred at 1000 rpm for 24 h. The volume fraction (X:Y) generally depends on the volume fraction of the BCP system. This fraction is calculated to solubilize both carbohydrate and synthetic blocks. For instance, in the present cases of $PS_{4.5k}$ -*b*-$MH_{1.3k}$, it is 70/30 (THF/water). There are two methods (A and B) of preparation (Fig. 4).

Example of Glyconanoparticles prepared from $PS_{4.5k}$-*b*-$MH_{1.3k}$

First, 5.0 mg **$PS_{4.5k}$-*b*-$MH_{1.3k}$** is dissolved in 5.0 g solvent mixture [70%:30%, (w/w), THF/H_2O] and stirred overnight. The polymer solution is sonicated for 10 min at 30 °C under 24 kHz and 10 W (amplitude adjustment at 100% and ultrasonic source operated in continuous mode) before use.

Method A: Two grams of the copolymer solution is slowly added dropwise to 100 g of Milli-Q water using a Pasteur pipet during a customized period of time (50 s to obtain monomodal spherical nanoparticles) under vigorous stirring at a stirring rate of 500 rpm. Subsequently, the

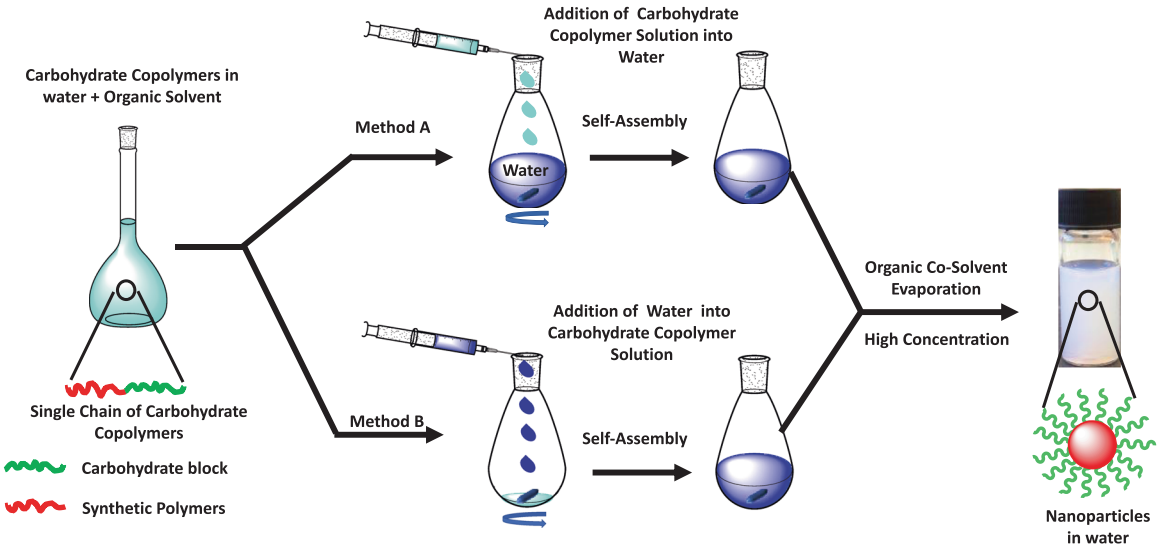

Fig. 4 Schematic illustration of the self-assembly procedure of $\mathbf{PS_{4.5k}}$-*b*-$\mathbf{MH_{1.3k}}$

suspension obtained from method A is stirred vigorously for 2 h, and THF is removed by evaporation under reduced pressure at room temperature.

Method B: Milli-Q water (100 g) is slowly added dropwise to 2.5 g of the copolymer solution in water using a Pasteur pipet for 10 min under vigorous stirring at a stirring rate of 500 rpm. Subsequently, the suspension obtained from method B is stirred vigorously for 2 h, and THF is removed by evaporation under reduced pressure at room temperature.

Characterization of the glyconanoparticles

Generally, imaging techniques such as atomic force microscopy (AFM), scanning electron microscopy (SEM), transmission electron microscopy (TEM) and light scattering are used to characterize nanoparticle systems. Here, we choose to list a few examples using dynamic light scattering (DLS).

DLS experiments are carried out using an ALV/CGS-8FS/N069 goniometer, which consists of an ALV/LSE-5004 multiple-τ digital corrector with a 125 ns initial sampling time and a 35-mW HeNe linearly polarized laser operating at a wavelength of 632.8 nm. Nanoparticle suspensions are directly poured into quartz cells thermostatted at 25 ± 0.1 °C. In DLS, the relaxation time distributions are determined using CONTIN analysis of the autocorrelation functions, and the hydrodynamic diameters ($D_{h,DLS}$) are calculated using the Stokes-Einstein equation. The original suspensions of glyconanoparticles are diluted with Milli-Q water to reach generally 0.01 mg mL^{-1} and introduced into the chamber with a syringe.

Typical nanoparticle DLS experiments of carbohydrate-based $\mathbf{PS_{4.5k}}$-*b*-$\mathbf{MH_{1.3k}}$

The hydrodynamic radii of the nanoparticles made from methods A and B after filtration using a 0.8-μm MF Millipore membrane (mixed cellulose esters) are determined using DLS measurements at detection angles of 30–110°. Typical results are illustrated in Fig. 5. The results show that the nanoparticles prepared using method B are more monodispersed and larger than those prepared using method A.

Self-assembly in the solid state: highly nanostructured thin films obtained from $\mathbf{PS_{2.5k}}$-b-$\mathbf{MH_{1.3k}}$

To gain more insight into the morphology of $\mathbf{PS_{4.5k}}$-*b*-$\mathbf{MH_{1.3k}}$ in the thin film state, atomic force microscopy (AFM) was carried out in tapping mode. The thin film samples were prepared on a silicon substrate by spin-coating from a 2 wt % $\mathbf{PS_{4.5k}}$-*b*-$\mathbf{MH_{1.3k}}$ solution in anisole followed by various solvent mixtures of THF and H_2O annealing for different times ranging from 0.5 to 3 h. The thickness of the thin films was ~30 nm, as determined by Flimetrics (F20-UV film analyzer).

Considering the asymmetric structure of the BCP, the observed morphology should consist of perpendicularly oriented cylinder domains of MH blocks (minor component) in a matrix of PS blocks (major component). The PS blocks prefer THF rather than H_2O, and the MH blocks prefer H_2O over THF. Therefore, both the MH and PS blocks migrate equally to the polymer–vapor interface by annealing with H_2O–THF, resulting in hexagonally close-

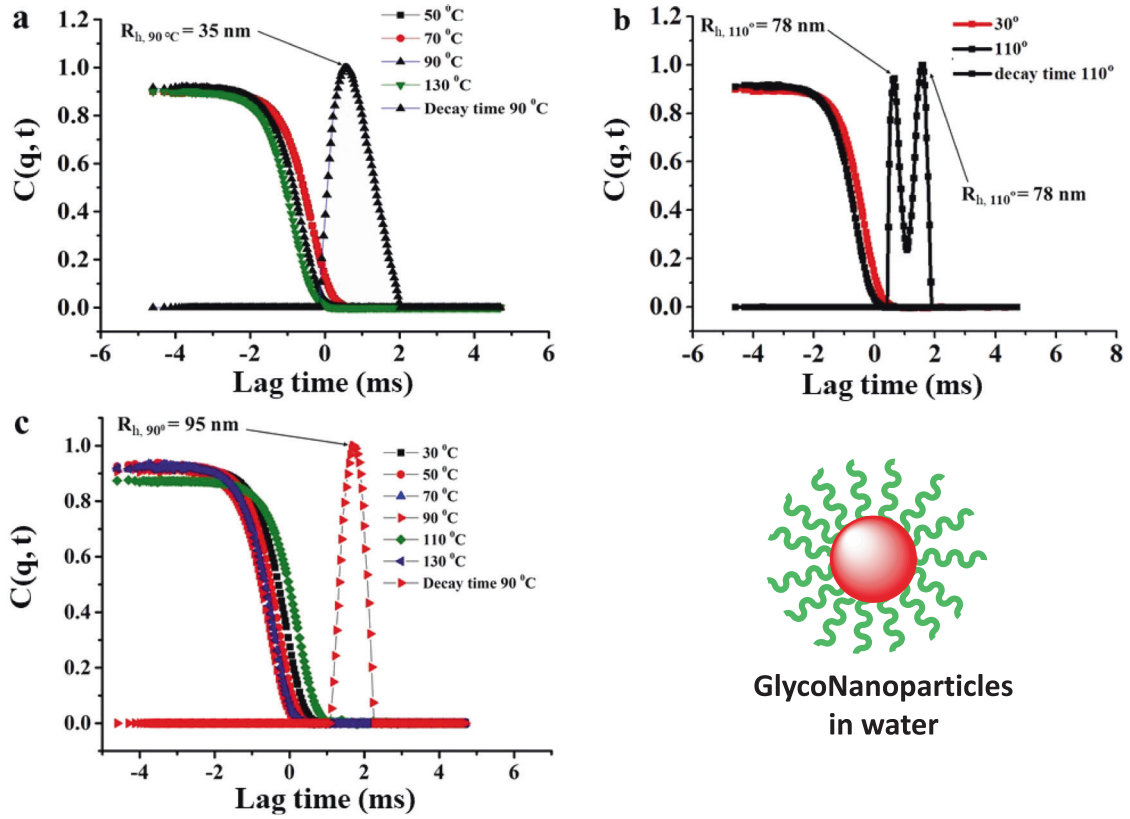

Fig. 5 Autocorrelation function C(q,t) measured in the range of 30–130 °C and decay time distribution at 30 °C, 90 °C, and 130 °C for the nanoparticles prepared from $\mathbf{PS_{4.5k}}$-***b***-$\mathbf{MH_{1.3k}}$ using method A (**a**, **b**) and method B (**c**)

packed MH cylinders oriented perpendicular to the surface. Equilibrium is reached after a certain time. As shown in Fig. 6, the surface morphologies of the annealed BCP thin films were characterized by AFM phase images. After 1 h of annealing time, a hexagonally close-packed cylinder perpendicularly oriented to the substrate was observed in the thin films after annealing with various solvent mixtures for different times. Such a difference in the surface morphologies of the BCP thin films due to the fraction of the annealing solvent was universally observed, indicating that the relative fractions of H_2O and THF in the annealing solvents are among the determining factors for the orientation of the cylinders. The white spots are carbohydrates, and the brown color represents the PS matrix. Interestingly, it is found that the cylinders of MH in a PS matrix are parallel to the substrate when the annealing time is 0.5 h for one case (9:1 THF/H2O), which we believe is a metastable morphology. At 1 h, the orientation of the cylinders is perpendicular to the substrate. Thus, not only χ but also selective evaporation, time of annealing, glass transition, and interaction with surfaces and substrates are of great importance.

Typical examples obtained on carbohydrate-based high-χ BCP systems are illustrated in Fig. 6 (e.g., MH-b-Block, where Block can be PS, PSSi, PDMS, PMMA, PI or P3HT) exhibits sub-10-nm nanodomains of hexagonal cylinders oriented perpendicular to the silicon substrate. Such systems have shown the lowest nanodomain size (5 nm) in the literature and have been applied successfully to the development, for example, of memory transistors [48, 50, 55, 56]. However, a strong limitation of these BCP systems is their lack of long-range ordering (although this can be improved by the use of directed self-assembly (DSA)) and the difficulty of controlling their perpendicular orientation over substrates other than silicon.

State-of-the-art systems thus afford self-assembled features as low as 5 nm from a handful of powerful high-χ BCP systems. In addition to this domain spacing aspect, the main actual Holy Grails in this domain are to efficiently manage the orientation of these features (both cylinders and lamellae oriented perpendicular to the substrate) and upgrade the long-range ordering of self-assembled nanostructures obtained from high-χ BCPs. Reaching and mastering these goals using straightforward, cost efficient and "green" methods would routinely afford sub-10 nm-scale ordered nanodomains that will have tremendous potential in nano (bio)electronic applications.

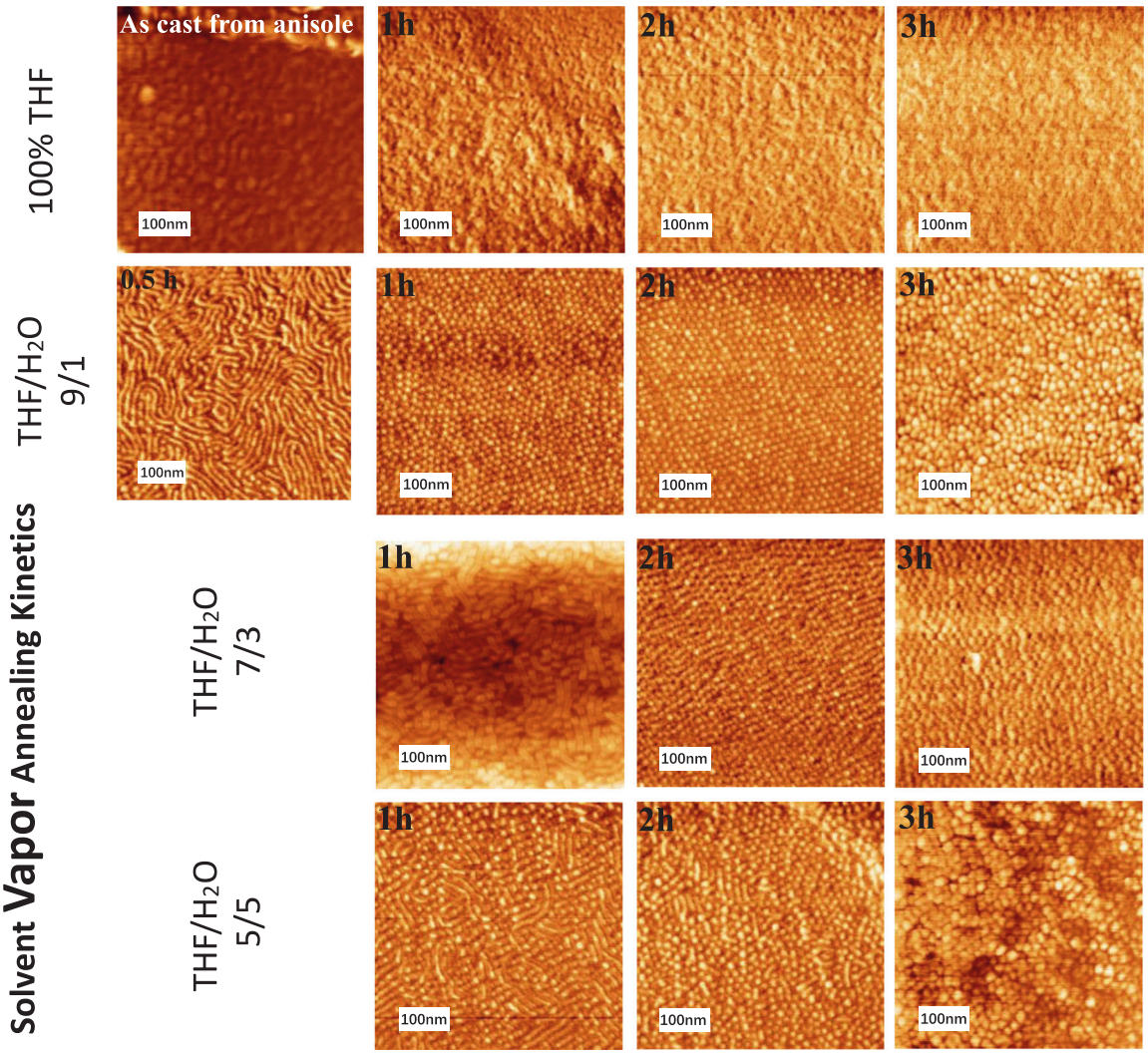

Fig. 6 AFM phase images of PS4.5K-b-MH1.3K thin films with a thickness of ~30 nm after solvent vapor annealing. The weight fraction of THF in the annealing mixture solvent (THF/H_2O) is shown. The annealing times from left to right are in the range of 0.5–3 h

Conclusion and perspectives

In this focused review paper, we have summarized the main results regarding the self-assembly of carbohydrate-based block copolymer systems (the so-called high χ) in solution (leading to the formation of glyconanoparticles) and in the solid-state (leading to highly nanostructured sub-10 nm thin films). We presented a simple strategy for driving the carbohydrate-based block copolymer system to form glyconanoparticles in solution whose size depends on the method of preparation. In water suspension, these nanoparticles are stable over many months and can be designed to fit the application targets in terms of size, encapsulation and decoration. The main advantage is that these glyconanoparticles carry sugar moieties as external shells and also carry OH groups that can be postfunctionalized to meet the application requirements. This paper also discusses the control of the orientation of the self-assembled thin film surface of BCPs using the solvent vapor annealing technique. In the asymmetrical specific PS-MH system, self-organized thin films formed by maltoheptaose-*block*-polystyrene, where the maltoheptaose (MH) block (minor component) likely assembles into cylindrical domains and the polystyrene (PS) block (major component) is the matrix, the orientation of the MH cylinders can be controlled by varying the composition of a miscible H_2O–THF mixture used as the annealing solvent. As concluded, the vapor produced from the H_2O–THF mixture is directly related to the mobility for both blocks of BCP, which is necessary to control the ordering of the self-assembled BCP thin films.

There are still important technological issues and bottlenecks in the fields of BCP self-assembly and in the design of controlled nanostructured thin films to be solved. Indeed,

most classical (petroleum) systems, such as the canonical PS-b-PMMA system, exhibit domain spacing >20 nm and will require downsizing of the periodic patterns using high-χ BCPs to reach sub-10-nm morphologies (such as carbohydrate-based BCP). In fact, only a few systems have been developed thus far that can reach features as small as 5 nm with periodic domains oriented perpendicular to the surface. The most important issues represent the major concerns of the community working in this highly international and competitive field and involve the pattern orientation and long-range order of self-assembled (high-χ) BCP thin films and the facile and selective degradation of one of the nanodomains.

Acknowledgements HL thanks the China Scholarship Council (CSC) for his scholarship support (grant #201806500007). RB and W.-C.C thank the CNRS, Univ Grenoble Alpes and NTU for their financial support of the IRP (International Research Project: Green Material Institute- France-Taiwan). This work was also financially supported by a JSPS Grant-in-Aid for Scientific Research (B) (No. 20H02792, No. 19H02769), JSPS Fund for the Promotion of Joint International Research (Fostering Joint International Research (B)) (No. 21KK0096), the Photoexcitonix Project (Hokkaido University), and the Creative Research Institute (Hokkaido University). The NanoBio-ICMG platforms (FR 2607) are acknowledged for their support for NMR block copolymer characterization and AFM for the different thin films.

Compliance with ethical standards

Conflict of interest The authors declare no competing interests.

Publisher's note Springer Nature remains neutral with regard to jurisdictional claims in published maps and institutional affiliations.

References

1. Liddle JA, Gallatin GM. Nanomanufacturing: a perspective. ACS Nano. 2016;10:2995–3014.
2. Nie Z, Kumacheva E. Patterning surfaces with functional polymers. Nat Mater. 2008;7:277–90.
3. Chai J, Buriak JM. Using cylindrical domains of block copolymers to self-assemble and align metallic nanowires. ACS Nano. 2008;2:489–501.
4. Hamley IW. Angew Chem Int Ed. 2003;42:1692–712.
5. Bates FS, Fredrickson GH. Block copolymer thermodynamics: theory and experiment. Ann Rev Phys Chem 1990;41:525–57.
6. Bang J, Jeong U, Ryu DY, Russell TP, Hawker CJ. Block copolymer nanolithography: translation of molecular level control to nanoscale patterns. Adv Mater. 2009;21:4769–92.
7. Kim SH, Misner MJ, Xu T, Kimura M, Russell TP. Nanostructured titania powders by hydrothermal processing and spray drying. Adv Mater. 2004;16:226–32.
8. Vayer M, Hillmyer MA, Dirany M, Thevenin G, Erre R, Sinturel C. Perpendicular orientation of cylindrical domains upon solvent annealing thin films of polystyrene-b-polylactide. Thin Solid Films. 2010;518:3710–5.
9. Yin J, Yao X, Liou J-Y, Sun W, Sun Y-S, Wang Y. Membranes with highly ordered straight nanopores by selective swelling of fast perpendicularly aligned block copolymers. ACS Nano. 2013;7:9961–74.
10. Bates CM, Maher MJ, Janes DW, Ellison CJ, Willson CG. Block Copolymer Lithography. Macromolecules. 2014;47:2–12.
11. Jung YS, Ross CA. Orientation-controlled self-assembled nanolithography using a polystyrene−polydimethylsiloxane block copolymer. Nano Lett 2007;7:2046–50.
12. Jeong JW, Park WI, Kim M-J, Ross CA, Jung YS. Highly tunable self-assembled nanostructures from a poly(2-vinylpyridine-b-dimethylsiloxane) block copolymer. Nano Lett. 2011;11:4095–101.
13. Aissou K, Nunns A, Manners I, Ross CA. Small. 2013, https://doi.org/10.1002/smll.201300657.
14. Sinturel C, Bates FS, Hillmyer MA. High χ–LowNBlock polymers: how far can we go. ACS Macro Lett. 2015;4:1044–50.
15. Otsuka I, Tallegas S, Sakai Y, Rochas C, Halila S, Fort S, et al. Control of 10 nm scale cylinder orientation in self-organized sugar-based block copolymer thin films. Nanoscale. 2013;5:2637–41.
16. Otsuka I, Zhang Y, Isono T, Rochas C, Kakuchi T, Satoh T, et al. Sub-10 nm scale nanostructures in self-organized linear di- and triblock copolymers and miktoarm star copolymers consisting of maltoheptaose and polystyrene. Macromolecules. 2015;48:1509–17.
17. Cushen JD, Otsuka I, Bates CM, Halila S, Fort S, Rochas C, et al. Oligosaccharide/silicon-containing block copolymers with 5 nm features for lithographic applications. ACS Nano. 2012;6:3424–33.
18. Luo Y, Montarnal D, Kim S, Shi W, Barteau KP, Pester CW, et al. Poly(dimethylsiloxane-b-methyl methacrylate): a promising candidate for sub-10 nm patterning. Macromolecules. 2015;48:3422–30.
19. Rho Y, Aissou K, Mumtaz M, Kwon W, Pécastaings G, Mocuta C, et al. Laterally ordered sub-10 nm features obtained from directed self-assembly of si-containing block copolymer thin films. Small. 2015;11:6377–83.
20. Aissou K, Mumtaz M, Fleury G, Portale G, Navarro C, Cloutet E, et al. Sub-10 nm features obtained from directed self-assembly of semicrystalline polycarbosilane-based block copolymer thin films. Adv Mater. 2015;27:261–5.
21. Kennemur JG, Justin G, Yao L, Bates FS, Hillmyer MA. Sub-5 nm Domains in Ordered Poly(cyclohexylethylene)-block-poly(methyl methacrylate) Block Polymers for Lithography. Macromolecules. 2014;47:1411–8.
22. Gross AJ, Chen X, Giroud F, Travelet C, Borsali R, Cosnier S. Redox-active glyconanoparticles as electron shuttles for mediated electron transfer with bilirubin oxidase in solution. J Am Chem Soc 2017;139:16076–9.
23. Hammond JL, Gross AJ, Giroud F, Travelet C, Borsali R, Cosnier S. Solubilized enzymatic fuel cell (SEFC) for quasi-continuous operation exploiting carbohydrate block copolymer glyconanoparticle mediators. ACS Energy Lett 2019;4:142–48.
24. Carrière M, Buzzetti PHM, Gorgy K, Mumtaz M, Travelet C, Borsali R, et al. Functionalizable glyconanoparticles for a versatile redox platform. Nanomaterials. 2021;11:1162.
25. Zepon KM, Otsuka I, Bouilhac C, Curti Muniz E, Soldi V, Borsali R. Self-assembly of oligosaccharide-b-PMMA block copolymer systems: glyco-nanoparticles and their degradation under UV exposure. Langmuir. 2016;32:4538–45. https://doi.org/10.1021/Acs.Langmuir.6b00212.
26. Isono T, Miyachi K, Satoh Y, Nakamura R, Zhang Y, Otsuka I, et al. Self-assembly of maltoheptaose-block-polycaprolactone copolymers: carbohydrate-decorated nanoparticles with tunable morphology and size in aqueous media. Macromolecules. 2016;49:4178–4194.
27. Gross AJ, Haddad R, Travelet C, Reynaud E, Audebert P, Borsali R, et al. Redox-active carbohydrate-coated nanoparticles: self-assembly of a cyclodextrin-polystyrene glycopolymer with

tetrazine-naphthalimide. Langmuir. 2016;32:11939–45. https://doi.org/10.1021/Acs.Langmuir.6b03512.
28. Zepon KM, Otsuka I, Bouilhac C, Curti Muniz E, Soldi V, Borsali R. Glyco-nanoparticles made from self-assembly of maltoheptaose-block-poly(methyl methacrylate): micelle, reverse micelle, and encapsulation. Biomacromolecules. 2015;16:2012–24.
29. Mazzarino L, Otsuka I, Halila S, Bubniak Ldos S, Mazzucco S, Santos-Silva MC, et al. Xyloglucan-block-poly(ϵ-caprolactone) copolymer nanoparticles coated with chitosan as biocompatible mucoadhesive drug delivery system. Macromol Biosci. 2014;14:709–19.
30. Otsuka I, Osaka M, Sakai Y, Travelet C, Putaux JL, Borsali R. Self-assembly of maltoheptaose-block-polystyrene into micellar nanoparticles and encapsulation of gold nanoparticles. Langmuir. 2013;29:15224–30.
31. Aissou K, Pfaff A, Giocomelli C, Travelet C, Mueller A, Borsali R. Fluorescent vesicles consisting of galactose-based amphiphilic copolymers with a π-conjugated sequence self-assembled in water. Macromol Rapid Commun. 2011;32:912–6.
32. Löfstrand A, Jafari Jam R, Mothander K, Nylander T, Mumtaz M, Vorobiev A, et al. Poly(styrene)-block-maltoheptaose films for sub-10 nm pattern transfer: implications for transistor fabrication. ACS Appl Nano Mater. 2021;4:5141–51.
33. Sakai-Otsuka Y, Ogawa Y, Satoh T, Chen WC, Borsali R. Carbohydrate-attached fullerene derivative for selective localization in ordered carbohydrate-block-poly(3-hexylthiophene) nanodomains. Carbohydr Polym. 2021;255:117528.
34. Sakai-Otsuka Y, Nishiyama Y, Putaux JL, Brinkmann M, Satoh T, Chen WC, et al. Competing molecular packing of blocks in a lamella-forming carbohydrate-block-poly(3-hexylthiophene) copolymer. Macromolecules. 2021;53:9054–64.
35. Mumtaz M, Takagi Y, Mamiya H, Tajima K, Bouilhac C, Isono T. et al. Sweet pluronic poly(propylene oxide)-b-oligosaccharide block copolymer systems: toward sub-4 nm thin-film nanopattern resolution. Eur Polym J. 2020;134:109831
36. Tammelin T, Abburi R, Gestranius M, Laine C, Setälä H, Österberg M. Correlation between cellulose thin film supramolecular structures and interactions with water. Adv Mater Interfaces, 2020;7:1901737–82.
37. Chuang TH, Chiang YC, Hsieh HC, Isono T, Huang CW, Borsali R, et al. Nanostructure- and orientation-controlled resistive memory behaviors of carbohydrate-block-polystyrene with different molecular weights via solvent annealing. ACS Appl Mater Interfaces. 2020;12:23217–24.
38. Isono T, Kawakami N, Watanabe K, Yoshida K, Otsuka I, Mamiya H, et al. Microphase separation of carbohydrate-based star-block copolymers with sub-10 nm periodicity. Polym Chem. 2019;10:1119–29.
39. Isono T, Komaki R, Lee C, Kawakami N, Ree BJ, Watanabe K, et al. Rapid access to discrete and monodisperse block co-oligomers from sugar and terpenoid toward ultrasmall periodic nanostructures. Commun Chem. 2020;3:135.
40. Hung CC, Nakahira S, Chiu YC, Isono T, Wu HC, Watanabe K, et al. Control over molecular architectures of carbohydrate-based block copolymers for stretchable electrical memory devices. Macromolecules. 2018;51:4966–75.
41. Yoshida K, Tanaka S, Yamamoto T, Tajima K, Borsali R, Isono T, et al. Chain-end functionalization with a saccharide for 10 nm microphase separation: "Classical" PS-b-PMMA versus PS-b-PMMA-saccharide. Macromolecules. 2018;51:8870–7.
42. Isono T, Nakahira S, Hsieh H-C, Katsuhara S, Mamiya H, Yamamoto T, et al. Carbohydrates as hard segments for sustainable elastomers: carbohydrates direct the self-assembly and mechanical properties of fully bio-based block copolymers. Macromolecules. 2020;53:5408–17.
43. Isono T, Ree BJ, Tajima K, Borsali R, Satoh T. Highly ordered cylinder morphologies with 10 nm scale periodicity in biomass-based block copolymers. Macromolecules. 2018;51:428–437.
44. Hung CC, Chiu YC, Wu HC, Lu C, Bouilhac C, Otsuka I, et al. Conception of stretchable resistive memory devices based on nanostructure-controlled carbohydrate-block-polyisoprene block copolymers. Adv Funct Mater. 2017;27:1–10.
45. Sakai-Otsuka Y, Zaioncz S, Otsuka I, Halila S, Rannou P, Borsali R. Self-assembly of carbohydrate-block-poly(3-hexylthiophene) diblock copolymers into sub-10 nm scale lamellar structures. Macromolecules. 2017;50:3365–76.
46. Liao Y, Chen WC, Borsali R. Carbohydrate-based block copolymer thin films: Ultrafast nano-organization with 7 nm resolution using microwave energy. Adv. Mater. 2017;1701645:1–6.
47. Otsuka I, Nilsson N, Suyatin DB, Maximov I, Borsali R. Carbohydrate-based block copolymer systems: directed self-assembly for nanolithography applications. Soft Matter. 2017;13:7406–11.
48. Sakai-Otsuka Y, Zaioncz S, Otsuka I, Halila S, Rannou P, Borsali R. Self-assembly of carbohydrate-block-poly(3-hexylthiophene) diblock copolymers into sub-10 nm scale lamellar structures. Macromolecules. 2017;50:3365–76.
49. Noronha CM, Otsuka I, Bouilhac C, Rochas C, Barreto PLM, Borsali R. Self-assembly of maltoheptaose-b-PMMA block copolymer systems: 10 nm Resolution in thin film and bulk states. Carbohydr Polym. 2017;170:15–22.
50. Isono T, Otsuka I, Halila S, Borsali R, Kakuchi T, Satoh T. Sub-20 nm microphase-separated structures in hybrid block copolymers consisting of polycaprolactone and maltoheptaose. J Photopolym Sci Technol. 2015;28:635–42.
51. Chiu YC, Sun HS, Lee WY, Halila S, Borsali R, Chen WC. Oligosaccharide carbohydrate dielectrics toward high-performance non-volatile transistor memory devices. Adv Mater. 2015;27:6257–64.
52. Chiu C, Otsuka I, Halila S, Borsali R, Chen C. High-performance nonvolatile transistor memories of pentacence using the green electrets of sugar-based block copolymers and their supramolecules. Adv Funct Mater. 2014;24:4240–9.
53. Isono T, Otsuka I, Suemasa D, Rochas C, Satoh T, Borsali R, et al. Synthesis, self-assembly, and thermal caramelization of maltoheptaose-conjugated polycaprolactones leading to spherical, cylindrical, and lamellar morphologies. Macromolecules. 2013;46:8932–40.
54. Tallegas S, Baron T, Gay G, Aggrafeil C, Salhi B, Chevolleau T, et al. Block copolymer technology applied to nanoelectronics: Block copolymer technology applied to nanoelectronics. Phys Status Solidi C. 2013;10:1195–206.
55. Isono T, Otsuka I, Kondo Y, Halila S, Fort S, Rochas C, et al. Sub-10 nm nano-organization in AB2- and AB3-type miktoarm star copolymers consisting of maltoheptaose and polycaprolactone. Macromolecules. 2013;46:1461–9.
56. Otsuka I, Isono T, Rochas C, Halila S, Fort S, Satoh T, et al. 10 nm scale cylinder–cubic phase transition induced by caramelization in sugar-based block copolymers. ACS Macro Lett. 2012;1:1379–82.
57. Cushen JD, Otsuka I, Bates CM, Halila S, Fort S, Rochas C, et al. Oligosaccharide/silicon-containing block copolymers with 5 nm features for lithographic applications. ACS Nano. 2012;6:3424–33.
58. Aissou K, Otsuka I, Rochas C, Fort S, Halila S, Borsali R. Nano-organization of amylose-b-polystyrene block copolymer films doped with bipyridine. Langmuir. 2011;27:4098–103.

59. Kolb HC, Finn MG, Sharpless KB Angewandte Chemie, International Edition. 2001;40:2004–21. (Wiley-VCH Verlag GmbH).
60. Guo Z, Jin Y, Liang T, Liu Y, Xu Q, Liang X, et al. Synthesis, chromatographic evaluation and hydrophilic interaction/reversed-phase mixed-mode behavior of a "Click beta-cyclodextrin" stationary phase. J Chromatogr A. 2009;121:257–63.
61. Otsuka I, Fuchise K, Halila S, Fort S, Aissou K, Pignot-Paintrand I, et al. Thermoresponsive vesicular morphologies obtained by self-assemblies of hybrid oligosaccharide-block-poly(N-isopropylacrylamide) copolymer systems. Langmuir, 2010;26:2325–32.
62. Liao Y, Goujon LJ, Reynaud E, Halila S, Gibaud A, Wei B, et al. Self-assembly of copper-free maltoheptaose-block-polystyrene nanostructured thin films in real and reciprocal space. Carbohydr Polym. 2019;212:222–8.